

The Thermal Conductivity, Thermal Diffusivity, and Heat Capacity of Gaseous Argon

L. Sun,¹ J. E. S. Venart,^{1,2} and R. C. Prasad³

Received June 6, 2001

This paper presents new absolute measurements for the thermal conductivity and thermal diffusivity of gaseous argon obtained with a transient hot-wire instrument. Six isotherms were measured in the supercritical dense gas at temperatures between 296 and 423 K and pressures up to 61 MPa. A new analysis for the influence of temperature-dependent properties and residual bridge unbalance is used to obtain the thermal conductivity with an uncertainty of less than 1% and the thermal diffusivity with an uncertainty of less than 4%. Isobaric heat capacity results were derived from measured values of thermal conductivity and thermal diffusivity using a density calculated from an equation of state. The heat capacities presented here have a nominal uncertainty of 4% and demonstrate that this property can be obtained successfully with the transient hot wire technique over a wide range of fluid states. The technique will be useful when applied to fluids which lack specific heat data.

KEY WORDS: argon; dense gas; heat capacity; thermal conductivity; thermal diffusivity; transient hot-wire technique.

1. INTRODUCTION

Argon is probably the chemical element most often studied and used as a model system for many thermodynamic and thermophysical studies. For this reason, a large number of measurements of the thermal conductivity of argon have been reported, most being made using the transient hot-wire technique (e.g., Refs. 1–3). Measurements of the thermal diffusivity using

¹ Department of Mechanical Engineering, University of New Brunswick, P.O. Box 4400, Fredericton, New Brunswick, Canada E3B 5A3.

² To whom correspondence should be addressed. E-mail: jvenart@unb.ca

³ Department of Engineering, University of New Brunswick, Saint John, New Brunswick, Canada E2L 4L5.

this technique are limited and unfortunately restricted in accuracy. Thus, there is a need for further accurate measurements of the thermal conductivity and thermal diffusivity in the supercritical dense gas to complement the data available at lower temperatures and to evaluate techniques for the more accurate determination of thermal diffusivity and, thus, specific heat, by this method.

We report here new measurements of the thermal conductivity and thermal diffusivity of argon at temperatures from 296 to 423 K with pressures to 61 MPa. The thermal conductivity data have an uncertainty of less than 1%, while the thermal diffusivity and derived heat capacity data have an estimated uncertainty of about 4%.

2. METHOD

The transient hot-wire method is widely accepted as a primary instrument and the most accurate technique for fluid thermal conductivity measurement. Its use for thermal diffusivity has been limited, due to the lack of reproducibility of the results obtained. The ideal working equation for thermal conductivity is based on the transient solution of Fourier's law for an infinite line source [4]. The ideal temperature rise of the fluid at the wire-fluid interface, $r = a$, at time t is

$$\Delta T = \frac{q}{4\pi\lambda(\rho, T)} \ln \frac{4\alpha t}{a^2 C} \quad (1)$$

where

$$\Delta T = \Delta T_w + \Sigma \delta T_i \quad (2)$$

and $\Sigma \delta T_i$ are appropriate corrections to the measured temperature rise of the wire, ΔT_w ; q is the power per unit length to the wire; λ is the thermal conductivity; $\alpha = \lambda/(\rho C_p)$ is the thermal diffusivity; ρ is the density; C_p is the isobaric heat capacity; and $C = 1.781 \dots$ the exponential of Euler's constant. The thermal conductivity is determined from the slope of the linear regression fit of the ΔT -versus- $\ln(t)$ data set via Eq. (1) and is referred to a reference temperature [4],

$$T_{\text{ref}} = T_0 + \frac{1}{2} [\Delta T(t_1) + \Delta T(t_2)] \quad (3)$$

since over the measurement this property and that of the isobaric specific heat capacity vary. Here $\Delta T(t_1)$ and $\Delta T(t_2)$ represent the temperature differences at the commencement, t_1 , and end, t_2 , times of the fit interval.

The thermal diffusivity of the fluid is often (e.g., Ref. 3) obtained directly from the same measurements as the thermal conductivity through the use of Eq. (1) as

$$\alpha = \frac{a^2 C}{4t'} \exp[4\pi\lambda \Delta T(a, t')/q] \quad (4)$$

The thermal diffusivity, α , is determined from values of λ and ΔT and the fit of the line at an arbitrary time t' . Time t' is normally selected to be 1 s in most data reduction programs.

The changes with temperature of the thermophysical properties of the fluid cause the temperature difference to be expressed approximately as [4]

$$\Delta T = -\frac{1}{2}\chi \Delta T^2 + \frac{q}{4\pi\lambda(\rho, T_0)} \ln \frac{4\alpha t}{a^2 C} + \left(\frac{q}{4\pi\lambda}\right)^2 (\chi - \phi) \ln 4 \quad (5)$$

where the subscript 0 denotes the initial temperature and χ and ϕ are the temperature coefficients of the thermal conductivity and heat capacity, respectively.

In Eq. (5) the last term is generally much smaller than the second. Since

$$\Delta T \approx \frac{q}{4\pi\lambda} \ln \frac{4\alpha t}{a^2 C} \quad (6)$$

the ratio of the last term to the second term can be written

$$(\chi - \phi) \ln 4 / \chi \left(\ln \frac{4\alpha t}{a^2 C} \right)^2 \quad (7)$$

where the order of χ and ϕ is about -0.003 and that of $[\ln(4\alpha t/a^2 C)]^2$ approximately 100. The last term in Eq. (5) is thus less than 5% of the second term (i.e., generally less than 1 mK) and can be ignored for now.

Equation (5) can therefore be simplified as

$$\Delta T' = \Delta T \left(1 + \frac{1}{2}\chi \Delta T \right) = \frac{q}{4\pi\lambda_0} \ln \frac{(4\lambda_0/\rho_0 C_p) t}{a^2 C} = \frac{q}{4\pi\lambda_0} \ln \frac{4\alpha t}{a^2 C} \quad (8)$$

where $\Delta T'$ denotes the temperature rise after correcting for the influence of χ . If the temperature coefficient is known in advance, or can be determined from conductivity measurements, then the thermal diffusivity can be determined more accurately by Eq. (8) than by Eq. (4).

The influence on ΔT of the temperature variation of properties over the measurement period is only 10s of millikelvins but its influence on the experimental data for thermal diffusivity is very significant. This may be illustrated as follows: from Eq. (4),

$$\alpha_1 = \frac{a^2 C}{4t} e^{\frac{\Delta T \left[1 + \frac{1}{2} \chi (\Delta T_1 + \Delta T_2) \right]}{G}} \quad (9)$$

and from Eq. (8),

$$\alpha_2 = \frac{a^2 C}{4t} e^{\Delta T (1 + \frac{1}{2} \chi \Delta T) / G} \quad (10)$$

where $G = q / (4\pi\lambda_0)$.

For $t = 1$ s, $\Delta T = \Delta T_2$ and the relative difference between Eq. (9) and Eq. (10) is

$$\frac{(\alpha_1 - \alpha_2)}{\alpha_2} = \left(\frac{\alpha_1}{\alpha_2} - 1 \right) = e^{\frac{\chi \Delta T_1 \Delta T_2}{2G}} - 1 \quad (11)$$

Thus, in this work to determine the thermal diffusivity, values of thermal conductivity are first determined to obtain its temperature coefficient at the bath or reference temperature and these in turn are utilized to correct for χ and obtain the thermal diffusivity at the reference temperature. These values are next used, via the power dependency, to establish an effective bridge imbalance or zero offset-temperature difference and thus determine the precise, power-independent, value of thermal diffusivity at the reference temperature.

3. EXPERIMENT

The transient hot-wire technique was utilized. Two wires with a nominal diameter of 12.70 μm , each of a different length, were utilized to compensate for end effects. The wires were calibrated over the temperature and pressure ranges of measurement in situ. The actual diameter of the wire was determined with a scanning electron microscope (SEM) to be 13.06 μm . The wire specifications and calibration coefficients are given in Table I along with the purity of the argon.

The measurement circuit is shown in Fig. 1 [5], where HP3497A is a data acquisition/control unit, HP6625A is a dc power supply, HP3458A is an integrating voltmeter which provides integration for times of 0 up to 16667 ms, HP3437A is an external trigger unit, and C-MOS is a digital

Table I. Wire and Test Fluid Specifications

(a) Calibration equation: $R = a_0 + a_1T + a_2T^2 + bP$ [T ($^{\circ}\text{C}$), P (MPa)]		
(b) Wire specification and calibration coefficients; long and short wires		
Mass purity (%)	99.999	99.999
Length (m)	0.08549 ± 0.00001	0.03395 ± 0.00001
Diameter (μm)	13.06 ± 0.01	13.06 ± 0.01
R_0	64.0327	21.4107
a_1	0.249593	0.0833068
a_2	-5.08635×10^{-5}	-1.58719×10^{-5}
b	-1.75154×10^{-3}	-5.58667×10^{-4}
(c) Test fluid: argon ($M = 39.944$, with a mass purity of 99.999%)		
T_{cr} (150.86 K)	P_{cr} (5.00 MPa)	ρ_{cr} ($536 \text{ kg} \cdot \text{m}^{-3}$)

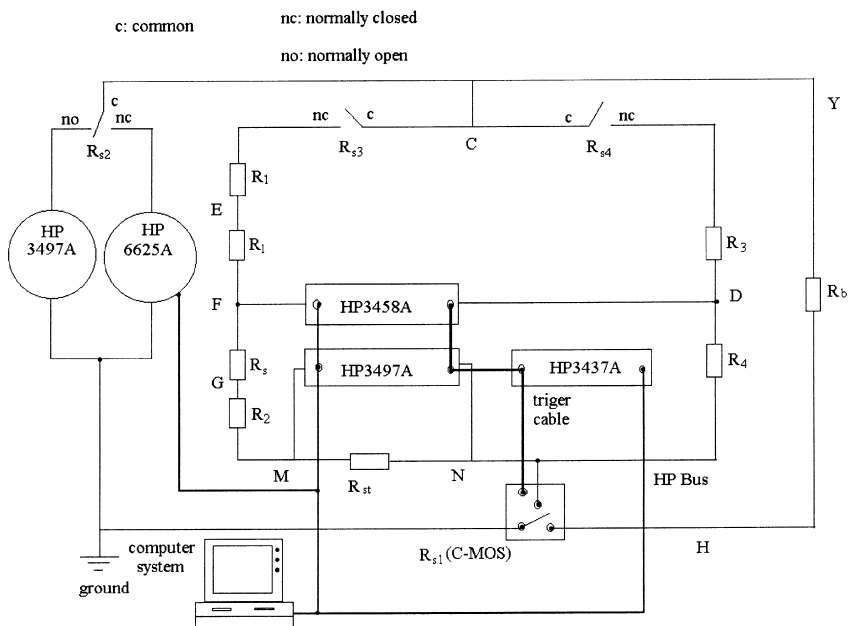


Fig. 1. Bridge circuit used for thermal conductivity and thermal diffusivity measurements [5]: R_i represents the resistance of the various bridge components, R_s is the resistance of the standard resistance, and R_l and R_s are the resistance of the long and short wires.

switch used to switch from the “dummy” to the “measurement” circuit. The HP3497A unit provides constant currents of 1, 0.1, and 0.01 mA, respectively, for use when calibrating the wires and balancing the bridge. The unit also provides an integrating voltmeter with integration times of 0.167, 1.67, and 16.67 ms and can provide digital and analogue switches used in the circuit, under computer control, during the preliminary balancing and final measurement processes. The HP6625A provides a high-stability fast-response dc power supply from 0 to 16 V for the heating of the wires. The HP3437A is used to provide an external signal to trigger the HP3497A, HP3458A, and C-MOS switch to connect the circuit and to trigger both the HP3497A and the HP3458A instruments to begin simultaneous measurements of both the current and the voltage across bridge elements.

The HP3497A is used to measure the voltage across the standard resistance, R_{st} , to determine the current through the hot wires. The unit is also utilized to provide a current of 1 mA when balancing the bridge. The HP3458A is used to measure the transient imbalance of the bridge, which is introduced by the temperature change of the hot wires, and to measure the voltages of every other branch of the bridge and the standard resistance.

Assume that the bridge is in an equilibrium state before a measurement and the power supply voltage from HP6625A is V_p ; then the transient imbalance voltage between F and D can be expressed as

$$\Delta V = \frac{V_p(R_l + R_1)}{R_1 + R_l + R_s + R_2 + R_{st}} - \frac{V_p R_3}{R_3 + R_4} \quad (12)$$

or

$$\Delta V = \frac{V_p R_4}{R_3 + R_4} - \frac{V_p(R_2 + R_s + R_{st})}{R_1 + R_l + R_s + R_2 + R_{st}} \quad (13)$$

By taking the average of these two expressions, we have

$$\Delta V = \Delta V_t + \delta V_1 + \delta V_2 \quad (14)$$

or

$$\Delta V = \frac{1}{2} \left[\frac{V_p(R_l + R_1 - R_s - R_2 - R_{st})}{R_l + R_1 + R_s + R_2 + R_{st}} + \frac{V_p(R_4 - R_3)}{R_3 + R_4} \right] = \Delta V_t + \delta V_1 + \delta V_2 \quad (15)$$

where

$$\Delta V_t = \frac{V_p}{2} \left(\frac{\Delta R_l - \Delta R_s}{R_l + R_1 + R_s + R_2 + R_{st}} \right) \quad (16)$$

and

$$\delta V_1 = \frac{V_p}{2} \left(\frac{R_{l0} + R_1 - R_{s0} - R_2 - R_{st}}{R_{l0} + R_1 + R_{s0} + R_2 + R_{st}} + \frac{R_4 - R_3}{R_3 + R_4} \right) = \frac{V_p}{2} F \quad (17)$$

$$\delta V_2 = \frac{V_p}{2} \left(\frac{R_{l0} + R_1 - R_{s0} - R_2 - R_{st}}{R_l + R_1 + R_s + R_2 + R_{st}} - \frac{R_{l0} + R_1 - R_{s0} - R_2 - R_{st}}{R_{l0} + R_1 + R_{s0} + R_2 + R_{st}} \right) \quad (18)$$

In the above expressions, ΔV_t is the transient imbalance voltage introduced by any temperature change of the hot wires, δV_1 is the voltage introduced by any imbalance of the bridge before the transient process, and δV_2 is the imbalance voltage introduced because of the resistance change of the branch—which actually is much smaller than δV_1 and can be ignored in this instance; F is a constant as the resistance of the bridge elements are known.

The above expression is based on the assumption that the voltmeter can measure the signal accurately. In reality, however, there are zero point errors (6 to 8 μV for the HP3458A voltmeter). Thus, Eq. (14) should have another term, i.e., a floating voltage, δV_f , and be rewritten

$$\Delta V = \Delta V_t + \delta V_1 + \delta V_2 + \delta V_f \quad (19)$$

To obtain accurate values of thermal conductivity and thermal diffusivity, all δV_i terms must be measured and taken into account.

To balance the bridge, a power level that changes linearly with time is applied to the circuit and the voltages between point F and point D, ΔV_p , and the voltage across the standard resistance, V_{st} , measured simultaneously. Thus, if the temperature rise of the hot wires, because of the applied power, can be ignored, the measured ΔV_p and V_{st} can be written

$$\Delta V_p = FV_p + \delta V_f = F_1 V_{st} + \delta V_f \quad (20)$$

Provided that the voltage across the standard resistance is measured, the imbalance of the bridge before testing and the unknown floating voltage of the voltmeter can be determined, provided that any heating effect of the wires is corrected.

Table II. Thermal Conductivity, Thermal Diffusivity, and Specific Heat of Argon

ID No.	T (K)	P (kPa)	ρ ($\text{kg}\cdot\text{m}^{-3}$)	q ($\text{W}\cdot\text{m}^{-1}$)	λ ($\text{W}\cdot\text{m}^{-1}\cdot\text{K}^{-1}$)	α ($10^{-8}\text{m}^2\cdot\text{s}^{-1}$)	C_p ($\text{J}\cdot\text{kg}^{-1}\cdot\text{K}^{-1}$)
	296.20	333	5.41314		0.01769^S		
AR2_300	297.893	333	5.38205	0.05658	0.01777 ^S		
AR3_300	299.969	333	5.34442	0.12747	0.01787 ^S		
	296.20	333	5.41314		0.01769^T		
AR2_300	299.161	333	5.35590	0.05658	0.01777 ^T		
AR3_300	302.787	333	5.29418	0.12747	0.01788 ^T		
	296.63	333	5.41009		0.01772	626.2	525.4
A20_3C1	298.304	333	5.37941	0.03181	0.01776		
A20_3D1	298.313	333	5.37924	0.03180	0.01774		
A20_3A2	299.594	333	5.35601	0.05655	0.01778		
A20_3B2	299.588	333	5.35611	0.05655	0.01776		
A20_3C2	301.199	333	5.32718	0.08847	0.01788		
A20_3D2	301.187	333	5.32739	0.08848	0.01789		
A20_3A3	303.246	333	5.29086	0.12761	0.01794		
A20_3B3	303.249	333	5.29080	0.12756	0.01793		
	296.18	882	14.3880		0.01800	233.9	534.8
A20_01A1	296.844	882	14.3550	0.01411	0.01799		
A20_01C1	297.679	882	14.3136	0.03177	0.01803		
A20_01A2	298.831	882	14.2569	0.05655	0.01807		
A20_01C2	300.299	882	14.1853	0.08844	0.01804		
	296.14	3757	62.3338		0.01913	53.22	576.7
A20_05C1	297.348	3757	62.0562	0.03179	0.01918		
A20_05A2	298.266	3757	61.8427	0.05654	0.01919		
A20_05C2	299.461	3757	61.5673	0.08839	0.01920		
A20_05A3	300.864	3757	61.2473	0.1274	0.01926		
A20_05C3	302.519	3757	60.8746	0.1735	0.01932		
	296.19	7106	119.821		0.02063	27.28	631.1
A20_10C1	297.248	7106	119.303	0.03179	0.02066		
A20_10A2	298.027	7106	118.923	0.05652	0.02066		
A20_10C2	299.046	7106	118.431	0.08837	0.02069		
A20_10A3	300.301	7106	117.832	0.12731	0.02070		
A20_10C3	301.705	7106	117.169	0.17344	0.02075		
	296.11	14534	249.710		0.02465	13.73	719.0
A20_20C1	296.905	14534	248.779	0.03179	0.02468		
A20_20A2	297.507	14534	248.083	0.05650	0.02461		
A20_20C2	298.293	14534	247.182	0.08829	0.02467		
A20_20A3	299.295	14534	246.045	0.12718	0.02465		
A20_20C3	300.394	14534	244.813	0.17315	0.02465		
A20_20A4	301.585	14534	243.494	0.22616	0.02465		
	296.20	20696	353.224		0.02870	10.38	782.8
A20_30C1	296.839	20696	352.129	0.03175	0.02863		
A20_30A2	297.347	20696	351.269	0.05643	0.02873		
A20_30C2	298.005	20696	350.163	0.08821	0.02861		

Table II. (Continued)

ID No.	T (K)	P (kPa)	ρ ($\text{kg}\cdot\text{m}^{-3}$)	q ($\text{W}\cdot\text{m}^{-1}$)	λ ($\text{W}\cdot\text{m}^{-1}\cdot\text{K}^{-1}$)	α ($10^{-8}\text{m}^2\cdot\text{s}^{-1}$)	C_p ($\text{J}\cdot\text{kg}^{-1}\cdot\text{K}^{-1}$)
A20_30A3	298.810	20696	348.821	0.12707	0.02861		
A20_30C3	299.709	20696	347.337	0.17299	0.02858		
A20_30A4	300.750	20696	345.637	0.22590	0.02852		
	296.27	27405	455.165		0.03296	8.693	833.6
A20_40C1	296.829	27405	453.962	0.03175	0.03284		
A20_40A2	297.271	27405	453.021	0.05642	0.03303		
A20_40C2	297.810	27405	451.879	0.08821	0.03286		
A20_40A3	298.485	27405	450.459	0.12703	0.03284		
A20_40C3	299.289	27405	448.781	0.17295	0.03279		
A20_40A4	300.159	27405	446.981	0.22579	0.03276		
	296.34	34298	545.316		0.03739	8.037	853.1
A20_50A2	297.196	34298	543.271	0.05642	0.03732		
A20_50C2	297.678	34298	542.126	0.08818	0.03729		
A20_50A3	298.277	34298	540.711	0.12696	0.03720		
A20_50C3	298.983	34298	539.053	0.17283	0.03714		
A20_50A4	299.793	34298	537.164	0.22561	0.03707		
A20_50C4	300.656	34298	535.167	0.28556	0.03701		
	296.37	41264	622.168		0.04162	7.738	864.5
A20_60A2	297.155	41264	620.214	0.05645	0.04148		
A20_60C2	297.585	41264	619.146	0.08819	0.04156		
A20_60A3	298.106	41264	617.857	0.12701	0.04144		
A20_60C3	298.727	41264	616.327	0.17283	0.04135		
A20_60A4	299.492	41264	614.453	0.22557	0.04128		
A20_60C4	300.211	41264	612.702	0.28543	0.04123		
	296.40	48019	685.166		0.04570	7.732	862.6
A20_70A2	297.117	48019	684.126	0.05639	0.04565		
A20_70C2	297.509	48019	682.370	0.08814	0.04547		
A20_70A3	297.986	48019	681.179	0.12696	0.04538		
A20_70C3	298.544	48019	679.791	0.17280	0.04531		
A20_70A4	299.198	48019	678.171	0.22553	0.04521		
A20_70C4	299.944	48019	676.331	0.28535	0.04512		
	296.42	55008	740.837		0.04962	7.822	856.3
A20_80A2	297.074	55008	739.221	0.05642	0.04962		
A20_80C2	297.437	55008	738.321	0.08814	0.04933		
A20_80A3	297.882	55008	737.220	0.12689	0.04931		
A20_80C3	298.415	55008	735.906	0.17269	0.04923		
A20_80A4	299.023	55008	734.412	0.22540	0.04914		
A20_80C4	299.714	55008	732.720	0.28520	0.04904		
	296.44	61916	788.442		0.05323	8.006	843.9
A20_90A2	297.093	61916	786.872	0.05638	0.05304		
A20_90B2	297.092	61916	786.873	0.05639	0.05315		
A20_90C2	297.415	61916	786.101	0.08810	0.05295		
A20_90D2	297.411	61916	786.106	0.08815	0.05308		

Table II. (Continued)

ID No.	T (K)	P (kPa)	ρ ($\text{kg}\cdot\text{m}^{-3}$)	q ($\text{W}\cdot\text{m}^{-1}$)	λ ($\text{W}\cdot\text{m}^{-1}\cdot\text{K}^{-1}$)	α ($10^{-8}\text{m}^2\cdot\text{s}^{-1}$)	C_p ($\text{J}\cdot\text{kg}^{-1}\cdot\text{K}^{-1}$)
A20_90A3	297.826	61916	785.117	0.12689	0.05300		
A20_90B3	297.819	61916	785.123	0.12688	0.05299		
A20_90C3	298.315	61916	783.940	0.17264	0.05291		
A20_90D3	298.311	61916	783.943	0.17267	0.05289		
A20_90A4	298.879	61916	782.592	0.22538	0.05283		
A20_90B4	298.874	61916	782.600	0.22532	0.05281		
A20_90C4	299.518	61916	781.068	0.28512	0.05268		
A20_90D4	299.516	61916	781.069	0.28509	0.05268		
	323.56	851	12.6783		0.01922	293.2	517.0
A50_01A1	324.283	851	12.6495	0.01550	0.01926		
A50_01C1	325.124	851	12.6161	0.03487	0.01930		
A50_01A2	326.305	851	12.5695	0.06202	0.01939		
A50_01A3	329.683	851	12.4382	0.13969	0.01957		
	323.58	3744	56.3300		0.02031	63.80	567.9
A50_05C1	324.853	3744	56.0896	0.03486	0.02037		
A50_05A2	325.814	3744	55.9096	0.06199	0.02041		
A50_05C2	327.061	3744	55.6778	0.09691	0.02047		
A50_05A3	328.516	3744	55.4100	0.13961	0.02052		
	323.58	7247	110.015		0.02168	32.06	614.7
A50_10C1	324.664	7247	109.588	0.03485	0.02169		
A50_10A2	325.523	7247	109.251	0.06197	0.02181		
A50_10C2	326.592	7247	108.836	0.09687	0.02182		
A50_10A3	327.889	7247	108.338	0.13953	0.02187		
A50_10C3	329.393	7247	107.764	0.18996	0.02194		
	323.58	14478	221.036		0.02503	16.81	674.3
A50_20C1	324.443	14478	220.279	0.03485	0.02504		
A50_20A2	325.112	14478	219.700	0.06196	0.02508		
A50_20C2	325.962	14478	218.969	0.09682	0.02513		
A50_20A3	327.020	14478	218.068	0.13947	0.02514		
A50_20C3	328.276	14478	217.009	0.18980	0.02515		
A50_20A4	329.616	14478	215.893	0.24783	0.02523		
	323.57	20924	316.061		0.02852	12.35	730.5
A50_30C1	324.303	20924	315.112	0.03483	0.02853		
A50_30A2	324.869	20924	314.389	0.06193	0.02856		
A50_30C2	325.573	20924	313.495	0.09676	0.02858		
A50_30A3	326.472	20924	312.362	0.13938	0.02858		
A50_30C3	327.520	20924	311.053	0.18969	0.02861		
A50_30A4	328.658	20924	309.647	0.24762	0.02863		
	323.53	27332	403.203		0.03212	10.48	760.5
A50_40A2	324.654	27332	401.382	0.06191	0.03213		
A50_40C2	325.263	27332	400.404	0.09671	0.03206		
A50_40A3	326.083	27332	399.095	0.13928	0.03208		
A50_40C3	326.984	27332	397.669	0.18958	0.03200		

Table II. (Continued)

ID No.	T (K)	P (kPa)	ρ ($\text{kg}\cdot\text{m}^{-3}$)	q ($\text{W}\cdot\text{m}^{-1}$)	λ ($\text{W}\cdot\text{m}^{-1}\cdot\text{K}^{-1}$)	α ($10^{-8}\text{m}^2\cdot\text{s}^{-1}$)	C_p ($\text{J}\cdot\text{kg}^{-1}\cdot\text{K}^{-1}$)
A50_40A4	327.967	27332	396.126	0.24750	0.03204		
A50_40C4	329.132	27332	394.316	0.31310	0.03203		
	323.55	34173	486.058		0.03582	9.218	799.6
A50_50A2	324.546	34173	484.204	0.06194	0.03581		
A50_50C2	325.1095	34173	483.157	0.09677	0.03579		
A50_50A3	325.786	34173	481.908	0.13930	0.03574		
A50_50C3	326.613	34173	480.391	0.18955	0.03576		
A50_50A4	327.529	34173	478.722	0.24739	0.03569		
A50_50C4	328.509	34173	476.952	0.31304	0.03573		
	323.59	41073	558.928		0.03948	8.688	813.0
A50_60A2	324.497	41073	557.089	0.06191	0.03942		
A50_60C2	324.993	41073	556.094	0.09674	0.03944		
A50_60A3	325.609	41073	554.864	0.13927	0.03944		
A50_60C3	326.307	41073	553.476	0.18950	0.03939		
A50_60A4	327.142	41073	551.826	0.24732	0.03940		
A50_60D4	328.106	41073	549.935	0.31289	0.03933		
	323.58	47921	621.771		0.04317	8.582	809.0
A50_70A2	324.407	47921	620.047	0.06188	0.04313		
A50_70C2	324.859	47921	619.106	0.09670	0.04309		
A50_70A3	325.406	47921	617.972	0.13917	0.04303		
A50_70C3	326.077	47921	616.587	0.18938	0.04298		
A50_70A4	326.857	47921	614.984	0.24714	0.04298		
A50_70C4	327.725	47921	613.210	0.31263	0.04289		
	323.59	54891	677.448		0.04669	8.544	806.6
A50_80A2	324.372	54891	675.801	0.06185	0.04664		
A50_80C2	324.775	54891	674.952	0.09665	0.04665		
A50_80A3	325.290	54891	673.870	0.13912	0.04651		
A50_80C3	325.905	54891	672.582	0.18935	0.04649		
A50_80A4	326.601	54891	671.130	0.24703	0.04647		
A50_80C4	327.404	54891	669.463	0.31245	0.04644		
	323.58	62173	728.377		0.05031	8.606	802.6
A50_90C2	324.673	62173	726.068	0.09661	0.05021		
A50_90A3	325.165	62173	725.036	0.13910	0.05017		
A50_90C3	325.729	62173	723.855	0.18931	0.05009		
A50_90A4	326.380	62173	722.497	0.24701	0.05002		
A50_90C4	327.129	62173	720.940	0.31247	0.04997		
A50_90A5	327.939	62173	719.263	0.38566	0.04991		
	347.46	864	11.9709		0.02026	320.9	527.4
A75_01C1	349.032	864	11.9162	0.03754	0.02039		
A75_01A2	350.220	864	11.8751	0.06673	0.02045		
A75_01C2	351.777	864	11.8216	0.10425	0.02055		
A75_01A3	353.761	864	11.7543	0.15014	0.02074		
	347.47	3884	54.1209		0.02135	70.54	559.2

Table II. (Continued)

ID No.	T (K)	P (kPa)	ρ ($\text{kg}\cdot\text{m}^{-3}$)	q ($\text{W}\cdot\text{m}^{-1}$)	λ ($\text{W}\cdot\text{m}^{-1}\cdot\text{K}^{-1}$)	α ($10^{-8}\text{m}^2\cdot\text{s}^{-1}$)	C_p ($\text{J}\cdot\text{kg}^{-1}\cdot\text{K}^{-1}$)
A75_05C1	348.760	3884	53.9052	0.03754	0.02144		
A75_05A2	349.738	3884	53.7435	0.06672	0.02148		
A75_05C2	351.063	3884	53.5261	0.10425	0.02164		
A75_05A3	352.519	3884	53.2894	0.15012	0.02165		
A75_05C3	354.222	3884	53.0153	0.20434	0.02180		
	347.47	7235	101.208		0.02254	37.10	600.3
A75_10C1	348.610	7235	100.835	0.03754	0.02260		
A75_10A2	349.466	7235	100.556	0.06672	0.02267		
A75_10C2	350.573	7235	100.198	0.10424	0.02276		
A75_10A3	351.955	7235	99.7553	0.15008	0.02285		
A75_10C3	353.475	7235	99.2732	0.20428	0.02294		
	347.45	14372	200.780		0.02555	19.63	648.2
A75_20C1	348.385	14372	200.121	0.03756	0.02562		
A75_20A2	349.068	14372	199.645	0.06679	0.02560		
A75_20C2	350.006	14372	198.996	0.10430	0.02565		
A75_20A3	351.138	14372	198.220	0.15021	0.02571		
A75_20C3	352.439	14372	197.336	0.20435	0.02574		
A75_20A4	353.945	14372	196.324	0.26669	0.02587		
	347.44	20548	283.550		0.02843	14.65	684.5
A75_30C1	348.248	20548	282.731	0.03755	0.02842		
A75_30A2	348.872	20548	282.101	0.06674	0.02852		
A75_30C2	349.646	20548	281.323	0.10424	0.02856		
A75_30A3	350.610	20548	280.361	0.15008	0.02860		
A75_30C3	351.750	20548	279.234	0.20426	0.02860		
A75_30A4	353.105	20548	277.908	0.26655	0.02870		
	347.44	27347	368.370		0.03169	11.70	735.2
A75_40A2	348.697	27347	366.722	0.06672	0.03171		
A75_40C2	349.367	27347	365.851	0.10423	0.03180		
A75_40A3	350.220	27347	364.748	0.15005	0.03184		
A75_40C3	351.204	27347	363.486	0.20416	0.03182		
A74_40A4	352.263	27347	362.138	0.26643	0.03188		
A75_40C4	353.639	27347	360.405	0.33704	0.03196		
	347.45	34385	447.650		0.03512	10.39	755.0
A75_50A2	348.561	34385	445.934	0.06668	0.03517		
A75_50C2	349.181	34385	444.984	0.10419	0.03515		
A75_50A3	349.918	34385	443.862	0.14999	0.03519		
A75_50C3	350.782	34385	442.553	0.20410	0.03520		
A75_50A4	351.800	34385	441.023	0.26631	0.03522		
A75_50C4	352.926	34385	439.345	0.33685	0.03528		
	347.46	41127	515.191		0.03835	9.640	772.2
A75_60A2	348.487	41127	513.457	0.06668	0.03835		
A75_60C2	349.025	41127	512.552	0.10417	0.03841		

Table II. (Continued)

ID No.	T (K)	P (kPa)	ρ ($\text{kg}\cdot\text{m}^{-3}$)	q ($\text{W}\cdot\text{m}^{-1}$)	λ ($\text{W}\cdot\text{m}^{-1}\cdot\text{K}^{-1}$)	α ($10^{-8}\text{m}^2\cdot\text{s}^{-1}$)	C_p ($\text{J}\cdot\text{kg}^{-1}\cdot\text{K}^{-1}$)
A75_60A3	349.691	41127	511.438	0.14998	0.03840		
A75_60C3	350.492	41127	510.104	0.20408	0.03840		
A75_60A4	351.421	41127	508.567	0.26628	0.03843		
A75_60C4	352.424	41127	506.918	0.33683	0.03844		
	347.47	48011	576.258		0.04166	9.364	782.0
A75_70A2	348.386	48011	574.624	0.06666	0.04167		
A75_70C2	348.914	48011	573.687	0.10417	0.04169		
A75_70A3	349.517	48011	572.620	0.14995	0.04164		
A75_70C3	350.256	48011	571.318	0.20403	0.04165		
A75_70A4	351.103	48011	569.834	0.26617	0.04169		
A75_70C4	352.108	48011	568.084	0.33674	0.04168		
	347.48	54955	630.732		0.04490	9.132	779.5
A75_80A2	348.351	54955	629.140	0.06663	0.04495		
A75_80C2	348.826	54955	628.273	0.10408	0.04482		
A75_80A3	349.391	54955	627.243	0.14984	0.04490		
A75_80C3	350.055	54955	626.038	0.20383	0.04485		
A75_80A4	350.890	54955	625.975	0.26597	0.04489		
A75_80C4	351.711	54955	623.054	0.33637	0.04488		
	347.46	62393	682.413		0.04823	9.118	775.1
A75_90A2	348.255	62393	680.945	0.06661	0.04822		
A75_90C2	348.699	62393	680.123	0.10407	0.04822		
A75_90A3	349.267	62393	679.075	0.14980	0.04827		
A75_90C3	349.861	62393	677.982	0.20383	0.04823		
A75_90A4	350.577	62393	676.669	0.26590	0.04822		
A75_90C4	351.411	62393	675.146	0.33630	0.04823		
	373.50	850	10.9438		0.02131	380.5	511.5
A10_01C1	375.125	850	10.8958	0.04048	0.02150		
A10_01A2	376.340	850	10.8601	0.07196	0.02159		
A10_01C2	377.970	850	10.8127	0.11238	0.02184		
A10_01A3	379.920	850	10.7565	0.16180	0.02200		
	373.51	3777	48.7255		0.02239	83.19	552.4
A10_05C1	374.870	3777	48.5392	0.04049	0.02252		
A10_05A2	375.860	3777	48.4042	0.07196	0.02253		
A10_05C2	377.150	3777	48.2296	0.11237	0.02267		
A10_05A3	378.650	3777	48.0282	0.16179	0.02279		
	373.50	7443	96.0523		0.02349	41.69	586.6
A10_10C1	374.670	7443	95.7202	0.04048	0.02362		
A10_10A2	375.565	7443	95.4687	0.07193	0.02369		
A10_10C2	376.700	7443	95.1519	0.11243	0.02384		
A10_10A3	378.130	7443	94.7560	0.16184	0.02401		
A10_10C3	379.805	7443	94.2969	0.22030	0.02416		
	373.48	14289	183.173		0.02607	22.81	624.0

Table II. (Continued)

ID No.	T (K)	P (kPa)	ρ ($\text{kg}\cdot\text{m}^{-3}$)	q ($\text{W}\cdot\text{m}^{-1}$)	λ ($\text{W}\cdot\text{m}^{-1}\cdot\text{K}^{-1}$)	α ($10^{-8}\text{m}^2\cdot\text{s}^{-1}$)	C_p ($\text{J}\cdot\text{kg}^{-1}\cdot\text{K}^{-1}$)
A10_20C1	374.450	14289	182.618	0.04051	0.02615		
A10_20A2	375.215	14289	182.184	0.07198	0.02624		
A10_20C2	376.220	14289	181.618	0.11239	0.02632		
A10_20A3	377.425	14289	180.944	0.16174	0.02646		
A10_20C3	378.850	14289	180.155	0.22001	0.02658		
A10_20A4	380.355	14289	179.330	0.28701	0.02668		
	373.51	20563	259.760		0.02876	16.48	671.8
A10_30C1	374.400	20563	259.027	0.04049	0.02889		
A10_30A2	375.045	20563	258.497	0.07193	0.02884		
A10_30C2	375.875	20563	257.818	0.11237	0.02888		
A10_30A3	376.900	20563	256.985	0.16177	0.02903		
A10_30C3	378.185	20563	255.950	0.22007	0.02913		
A10_30A4	379.405	20563	254.977	0.28701	0.02920		
	373.51	27364	337.542		0.03162	13.42	698.0
A10_40C1	374.285	27364	336.716	0.04046	0.03164		
A10_40A2	374.880	27364	336.082	0.07192	0.03176		
A10_40C2	375.640	27364	335.275	0.11234	0.03178		
A10_40A3	376.560	27364	334.305	0.16167	0.03186		
A10_40C3	377.610	27364	333.206	0.21989	0.03195		
A10_40A4	378.945	27364	331.821	0.28686	0.03201		
	373.52	34392	411.083		0.03464	11.83	712.3
A10_50A2	374.735	34392	409.535	0.07189	0.03471		
A10_50C2	375.430	34392	408.659	0.11229	0.03478		
A10_50A3	376.220	34392	407.667	0.16168	0.03485		
A10_50C3	377.185	34392	406.463	0.22000	0.03492		
A10_50A4	378.340	34392	405.033	0.28700	0.03502		
A10_50C4	379.435	34392	403.665	0.36296	0.03505		
	373.54	41046	474.022		0.03761	10.81	734.0
A10_60A2	374.655	41046	472.445	0.07191	0.03760		
A10_60C2	375.280	41046	471.568	0.11232	0.03779		
A10_60A3	376.015	41046	470.542	0.16173	0.03771		
A10_60C3	376.910	41046	469.299	0.21995	0.03779		
A10_60A4	377.900	41046	467.933	0.28696	0.03782		
A10_60C4	379.000	41046	465.199	0.36292	0.03787		
	373.55	48142	534.334		0.04054	10.19	744.5
A10_70A2	374.545	48142	532.826	0.07193	0.04060		
A10_70C2	375.120	48142	531.960	0.11232	0.04065		
A10_70A3	375.845	48142	530.872	0.16165	0.04077		
A10_70C3	376.695	48142	529.602	0.21984	0.04081		
A10_70A4	377.565	48142	528.310	0.28677	0.04087		
A10_70C4	378.600	48142	526.781	0.36259	0.04091		
	373.51	55906	593.143		0.04350	9.969	735.7

Table II. (Continued)

ID No.	T (K)	P (kPa)	ρ ($\text{kg}\cdot\text{m}^{-3}$)	q ($\text{W}\cdot\text{m}^{-1}$)	λ ($\text{W}\cdot\text{m}^{-1}\cdot\text{K}^{-1}$)	α ($10^{-8}\text{m}^2\cdot\text{s}^{-1}$)	C_p ($\text{J}\cdot\text{kg}^{-1}\cdot\text{K}^{-1}$)
A10_80A2	374.485	55906	591.596	0.07186	0.04359		
A10_80C2	374.980	55906	590.815	0.11229	0.04354		
A10_80A3	375.610	55906	589.824	0.16165	0.04366		
A10_80C3	376.380	55906	588.618	0.21995	0.04373		
A10_80A4	377.240	55906	587.276	0.28700	0.04377		
A10_80C4	378.325	55906	585.593	0.36300	0.04381		
	373.50	63144	641.987		0.04691	9.818	730.7
A10_90A2	374.395	63144	640.531	0.07190	0.04700		
A10_90C2	374.880	63144	639.747	0.11234	0.04692		
A10_90A3	375.470	63144	638.797	0.16169	0.04702		
A10_90C3	376.150	63144	637.705	0.22001	0.04706		
A10_90A4	376.930	63144	636.457	0.28696	0.04707		
A10_90C4	377.795	63144	635.079	0.36284	0.04714		
	398.73	897	10.8097		0.02253	395.2	527.3
A12_01A1	399.485	897	10.7891	0.01926	0.02263		
A12_01C1	400.375	897	10.7648	0.04333	0.02265		
A12_01A2	401.600	897	10.7316	0.07700	0.02274		
A12_01C2	403.180	897	10.6891	0.12023	0.02295		
	398.72	3772	45.4348		0.02338	95.99	536.1
A12_05C1	400.100	3772	45.2706	0.04333	0.02357		
A12_05A2	401.130	3772	45.1492	0.07699	0.02361		
A12_05C2	402.515	3772	44.9871	0.12024	0.02382		
A12_05A3	404.210	3772	44.7903	0.17303	0.02402		
	398.71	7410	89.0402		0.02451	48.02	573.2
A12_10C1	399.895	7410	88.7543	0.04332	0.02461		
A12_10A2	400.845	7410	88.5270	0.07699	0.02475		
A12_10C2	402.045	7410	88.2416	0.12027	0.02489		
A12_10A3	403.605	7410	87.8737	0.17302	0.02504		
A12_10C3	405.095	7410	87.5253	0.23532	0.02517		
	398.71	14250	169.468		0.02689	26.32	602.9
A12_20C1	399.755	14250	168.968	0.04335	0.02703		
A12_20A2	400.545	14250	168.592	0.07702	0.02701		
A12_20C2	401.550	14250	168.115	0.12030	0.02709		
A12_20A3	402.785	14250	167.535	0.17309	0.02722		
A12_20C3	404.330	14250	166.814	0.23551	0.02739		
	398.69	20563	240.652		0.02926	18.90	643.3
A12_30C1	399.600	20563	240.020	0.04333	0.02933		
A12_30A2	400.330	20563	239.517	0.07700	0.02948		
A12_30C2	401.200	20563	238.920	0.12026	0.02943		
A12_30A3	402.325	20563	238.154	0.17312	0.02956		
A12_30C3	403.620	20563	237.280	0.23546	0.02970		
A12_30A4	404.925	20563	236.405	0.30714	0.02983		

Table II. (Continued)

ID No.	T (K)	P (kPa)	ρ ($\text{kg}\cdot\text{m}^{-3}$)	q ($\text{W}\cdot\text{m}^{-1}$)	λ ($\text{W}\cdot\text{m}^{-1}\cdot\text{K}^{-1}$)	α ($10^{-8}\text{m}^2\cdot\text{s}^{-1}$)	C_p ($\text{J}\cdot\text{kg}^{-1}\cdot\text{K}^{-1}$)
	398.67	27655	315.766		0.03203	15.48	655.3
A12_40C1	399.495	27655	315.017	0.04334	0.03216		
A12_40A2	400.125	27655	314.449	0.07699	0.03211		
A12_40C2	400.890	27655	313.762	0.12025	0.03214		
A12_40A3	401.905	27655	312.855	0.17305	0.03230		
A12_40C3	403.100	27655	311.796	0.23539	0.03248		
A12_40A4	404.285	27655	310.754	0.30702	0.03244		
	398.66	34388	381.578		0.03478	13.63	668.7
A12_50C1	399.425	34388	380.760	0.04329	0.03492		
A12_50A2	399.990	34388	380.156	0.07696	0.03472		
A12_50C2	400.685	34388	379.416	0.12023	0.03489		
A12_50A3	401.580	34388	378.468	0.17308	0.03494		
A12_50C3	402.655	34388	377.336	0.23543	0.03499		
A12_50A4	403.810	34388	376.128	0.30708	0.03506		
	398.65	41169	442.251		0.03754	12.33	688.4
A12_60A2	399.880	41169	440.774	0.07696	0.03766		
A12_60C2	400.565	41169	439.955	0.12023	0.03756		
A12_60A3	401.365	41169	439.002	0.17302	0.03752		
A12_60C3	402.350	41169	437.835	0.23539	0.03768		
A12_60A4	403.485	41169	436.499	0.30705	0.03768		
A12_60C4	404.665	41169	435.119	0.38822	0.03774		
	398.68	48203	499.383		0.04029	11.67	691.3
A12_70A2	399.785	48203	497.942	0.07693	0.04040		
A12_70C2	400.420	48203	497.118	0.12022	0.04034		
A12_70A3	401.245	48203	496.051	0.17302	0.04037		
A12_70C3	402.020	48203	495.054	0.23540	0.04035		
A12_70A4	402.975	48203	493.831	0.30695	0.04048		
A12_70C4	404.060	48203	492.450	0.38813	0.04054		
	398.68	55009	549.542		0.04282	11.12	700.7
A12_80A2	399.720	55009	548.114	0.07693	0.04286		
A12_80C2	400.285	55009	547.341	0.12016	0.04282		
A12_80A3	400.995	55009	546.373	0.17294	0.04308		
A12_80C3	401.865	55009	545.193	0.23529	0.04301		
A12_80A4	402.750	55009	543.997	0.30687	0.04295		
A12_80C4	403.640	55009	542.801	0.38807	0.04309		
	422.14	867	9.86325		0.02346	463.8	512.8
A15_01C1	423.550	867	9.83014	0.03920	0.02364		
A15_01A2	424.655	867	9.80434	0.06967	0.02367		
A15_01C2	426.050	867	9.77197	0.10884	0.02383		
A15_01A3	427.795	867	9.73177	0.15664	0.02407		
	422.13	3801	43.1434		0.02424	103.5	542.3
A15_05C1	423.305	3801	43.0191	0.03920	0.02439		

Table II. (Continued)

ID No.	T (K)	P (kPa)	ρ ($\text{kg}\cdot\text{m}^{-3}$)	q ($\text{W}\cdot\text{m}^{-1}$)	λ ($\text{W}\cdot\text{m}^{-1}\cdot\text{K}^{-1}$)	α ($10^{-8}\text{m}^2\cdot\text{s}^{-1}$)	C_p ($\text{J}\cdot\text{kg}^{-1}\cdot\text{K}^{-1}$)
A15_05A2	424.225	3801	42.9224	0.06965	0.02450		
A15_05C2	425.395	3801	42.6961	0.10881	0.02464		
A15_05A3	426.850	3801	42.6490	0.15664	0.02483		
	422.16	7575	85.5828		0.02540	52.52	565.0
A15_10C1	423.245	7575	85.3491	0.03919	0.02550		
A15_10A2	424.030	7575	85.1806	0.06966	0.02560		
A15_10C2	425.075	7575	84.9574	0.10884	0.02568		
A15_10A3	426.400	7575	84.6761	0.15662	0.02584		
A15_10C3	427.900	7575	84.3602	0.21314	0.02598		
	422.24	14115	157.490		0.02745	29.31	594.6
A15_20C1	423.160	14115	157.113	0.03921	0.02751		
A15_20A2	423.860	14115	156.827	0.06970	0.02760		
A15_20C2	424.775	14115	156.454	0.10885	0.02774		
A15_20A3	425.865	14115	156.013	0.15669	0.02779		
A15_20C3	427.255	14115	155.467	0.21311	0.02793		
	422.24	20550	225.338		0.02969	21.33	617.7
A15_30C1	423.080	20550	224.835	0.03919	0.02977		
A15_30A2	423.690	20550	224.473	0.06968	0.02983		
A15_30C2	424.475	20550	224.008	0.10885	0.02989		
A15_30A3	425.460	20550	223.429	0.15662	0.02997		
A15_30C3	426.630	20550	222.745	0.21308	0.03010		
	422.22	27421	293.659		0.03204	16.79	649.8
A15_40C1	422.945	27421	293.099	0.03920	0.03209		
A15_40A2	423.515	27421	292.659	0.06965	0.03218		
A15_40C2	424.245	27421	292.097	0.10877	0.03222		
A15_40A3	425.140	27421	291.412	0.15661	0.03234		
A15_40C3	426.200	27421	290.605	0.21305	0.03243		
A15_40A4	427.480	27421	289.638	0.27794	0.03255		
	422.17	34327	357.504		0.03451	14.50	665.7
A15_50A2	423.360	34327	356.405	0.06961	0.03455		
A15_50C2	424.030	34327	355.788	0.10878	0.03472		
A15_50A3	424.840	34327	355.045	0.15662	0.03479		
A15_50C3	425.790	34327	354.178	0.21301	0.03486		
A15_50A4	426.960	34327	353.116	0.27791	0.03498		
A15_50C4	427.925	34327	352.247	0.35149	0.03500		
	422.17	41266	416.537		0.03715	13.17	677.2
A15_60A2	423.270	41266	415.382	0.06962	0.03724		
A15_60C2	423.870	41266	414.755	0.10876	0.03723		
A15_60A3	424.610	41266	413.985	0.15656	0.03728		
A15_60C3	425.420	41266	413.146	0.21297	0.03728		
A15_60A4	426.425	41266	412.110	0.27787	0.03738		
A15_60C4	427.485	41266	411.024	0.35145	0.03745		

Since a series of small voltages is used to determine F_1 and δV_f , some self-heating of the wire will result. First, assume that the power supply voltage can be written

$$V_p = V_{pe} \frac{t}{t_e} \quad (21)$$

where A is a constant and t is the elapsed time. The energy input can be written

$$q = q_e \left(\frac{t}{t_e} \right)^2 \quad (22)$$

where the subscript e denotes the value at the termination of the procedure and t is the time. Therefore, the temperature rise can be approximated as

$$\delta T = \frac{q_e}{4\pi\lambda_1} \left(\frac{t}{t_e} \right)^2 + \frac{q_e}{4\pi\lambda_2} \left(\frac{t}{t_e} \right)^2 \left(\ln \frac{4k_2 t}{a^2 C} - \frac{3}{2} \right) \quad (23)$$

and the error introduced in F_1 can be corrected.

4. RESULTS

The thermal conductivity and thermal diffusivity of argon were measured along six nominal isotherms, 296, 323, 348, 373, 398, and 423 K, at pressures to 61 MPa. The measurements are listed in Table II along with their corresponding equilibrium values. The density values were obtained using the NIST SRD Database 14 [6]. Over 340 individual experimental data points for thermal conductivity are used to establish 62 determinations of thermal diffusivity and specific heat. The derived values of thermal conductivity, thermal diffusivity, and specific heat at the established reference temperatures are indicated in boldface type in Table II. The influence of thermal radiation was estimated using Eq. (8) of Ref. 2 to be less than 0.2% for thermal conductivity and less than 1% for thermal diffusivity.

4.1. Thermal Conductivity

The thermal conductivity values were correlated with an equation of the form

$$\lambda(\text{W} \cdot \text{m} \cdot \text{K}^{-1}) = \lambda_0 + a_0 + a_1 \rho(\text{kg} \cdot \text{m}^{-3}) + a_2 (\rho(\text{kg} \cdot \text{m}^{-3}))^2 \quad (24)$$

Table III. Coefficients for Eqs. (24) and (25)

a_0	a_1	a_2	b_0	b_1	b_2
1.1212×10^{-4}	2.0516×10^{-5}	2.9472×10^{-8}	2.9946×10^{-3}	5.7376×10^{-5}	-2.2458×10^{-8}

where λ_0 is the ideal gas thermal conductivity of argon, obtained by extrapolating the measured thermal conductivity to zero density with the values fit versus temperature as

$$\lambda_0 = b_0 + b_1(T(\text{K})) + b_2(T(\text{K}))^2 \quad (25)$$

The coefficients for Eqs. (24) and (25) are listed in Table III.

The thermal conductivities from this work and other sources are shown in Fig. 2. The deviations of all the data from Eq. (24) are indicated in Fig. 3. Figure 3 shows that the maximum deviation in the thermal conductivity of the present work from Eq. (24) is about 2.5%, with a standard deviation of about 0.9%.

The data of Perkins et al. [2] were also obtained using a transient hot-wire technique (300 K, 2 to 65 MPa) with a claimed uncertainty of 1%. Figure 3 shows that the data deviate from Eq. (24) by 2 to 3% in the

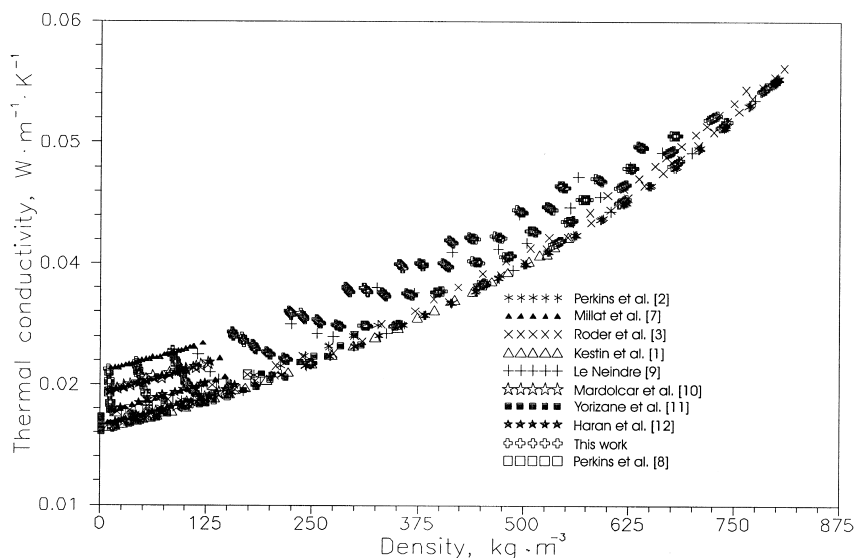


Fig. 2. Thermal conductivity of argon as a function of density as represented by Eq. (24).

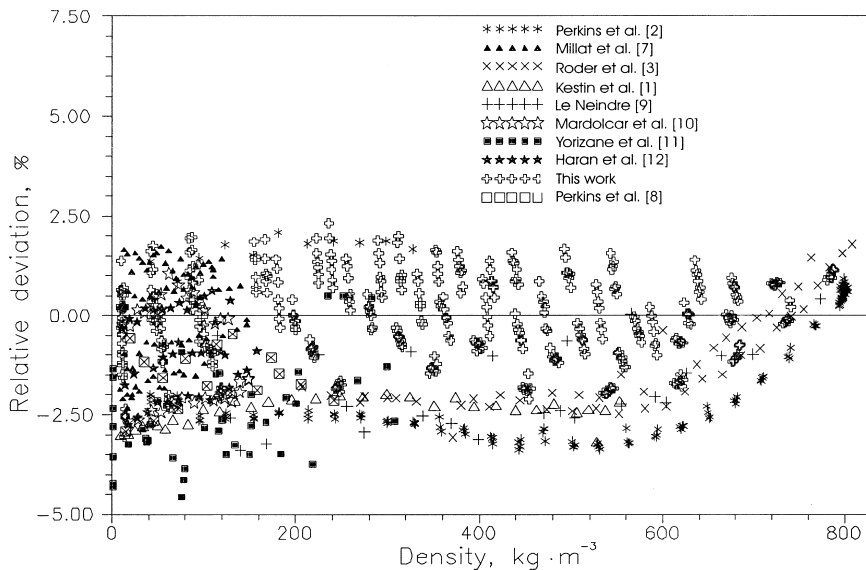


Fig. 3. Deviations of the thermal conductivity of argon from Eq. (24).

regions of both low and high densities, respectively. The data obtained by Millat et al. [7] were also measured with a transient hot-wire technique with a claimed uncertainty of 1%. In Fig. 3 it can be seen that the maximum deviation for this set of data is less than 3%, with most data deviating less than 2%. The data obtained by Roder et al. [3] and Perkins et al. [8] were measured using a transient hot-wire technique (103 to 324 K, 0 to 67 MPa) with a claimed accuracy of 1%. In the low-density region, their data [3, 8] fall below those given by Eq. (24), and in the high-density region, the deviations are greater: however, the maximum deviation overall is less than 2.5%. The data obtained by Kestin et al. [1] were measured using a hot-wire technique (298 to 303 K, 0 to 35 MPa) with a claimed uncertainty better than 1%. These data are 3% less than those given by Eq. (24) in the low-density region but somewhat higher in the high-density region. Data of le Neindre [9] were obtained using a steady-state coaxial cylinder instrument (298 to 1000 K, 0.1 to 100 MPa) with a claimed uncertainty of 3%. In the high-density region the maximum deviation from Eq. (24) is less than 2%, and in the low-density region the data deviate by greater than 3%. The data obtained by Mardolcar et al. [10] were measured by a transient hot-wire technique (107 to 423 K, 0 to 10 MPa) with an estimated uncertainty of 0.5%. In Fig. 3, it can be seen that the maximum deviation from Eq. (24) is less than 2%. The data obtained by Yorzane et al. [11] were measured using a vertical coaxial cylindrical cell

(298 to 323 K, 0.1 to 20 MPa) with an estimated uncertainty of only 3%. Figure 3 shows that there is a maximum deviation of 4%. The data obtained by Haran et al. [12] were measured with a transient hot-wire technique (300 to 430 K, 0 to 10 MPa) with an estimated uncertainty of 0.5%. In Fig. 3, it can be seen that the maximum deviation is as large as 2%.

From the comparisons above, it can be seen that within the temperature and pressure ranges considered, the maximum deviation among the thermal conductivity data for argon obtained by the different authors is less than 4% compared with the correlation given by Eq. (24). Most of the data sets from the literature deviate by less than 2% from the correlation. The data from these experiments indicate a reproducibility of 0.5% for each transient hot-wire instrument.

4.2. Thermal Diffusivity

The thermal diffusivity values obtained along six isotherms and those from the literature are shown in Fig. 4 as a function of density. Figure 4 shows that the thermal diffusivity of argon changes very sharply with density in the low-density region.

To compare the reproducibility of these data with those from the literature, we compare the deviations of the thermal diffusivity data from the values derived using the NIST SRD Database 14 [6] in Fig. 7. It can be seen that the thermal diffusivity results of Perkins et al. [2] exhibit very

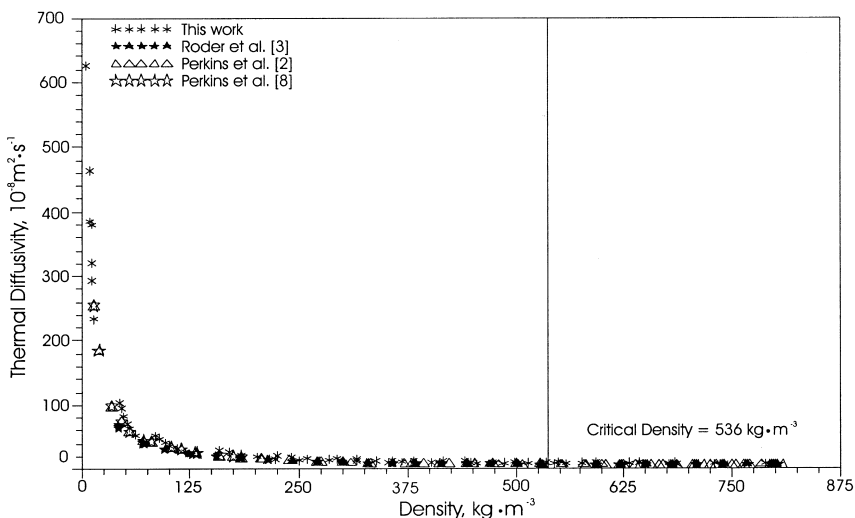


Fig. 4. Thermal diffusivity of argon as a function of density.

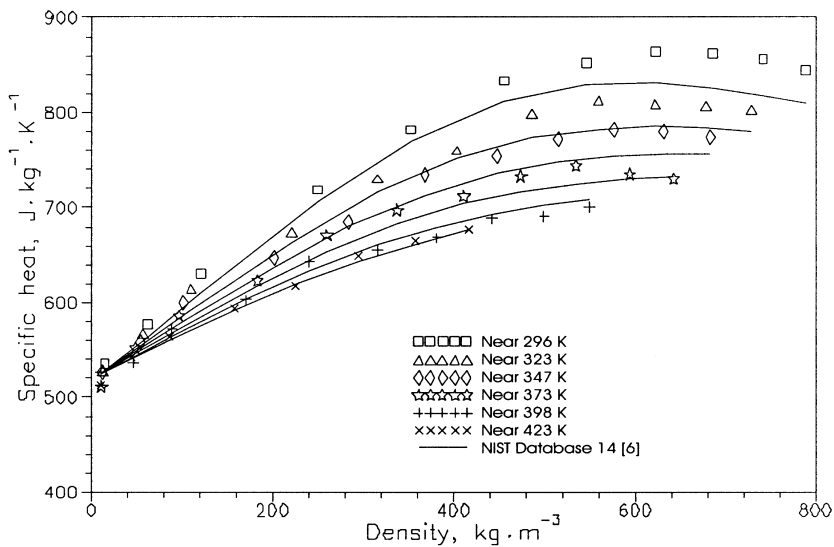


Fig. 5. Isobaric specific heat of argon as a function of density; present work.

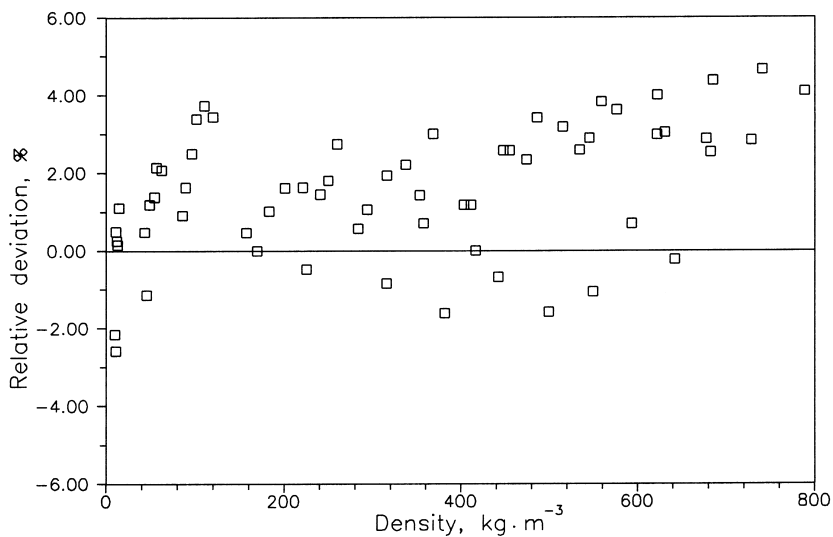


Fig. 6. Deviations of the derived isobaric specific heat for argon compared to the NIST SRD Database 14 [6].

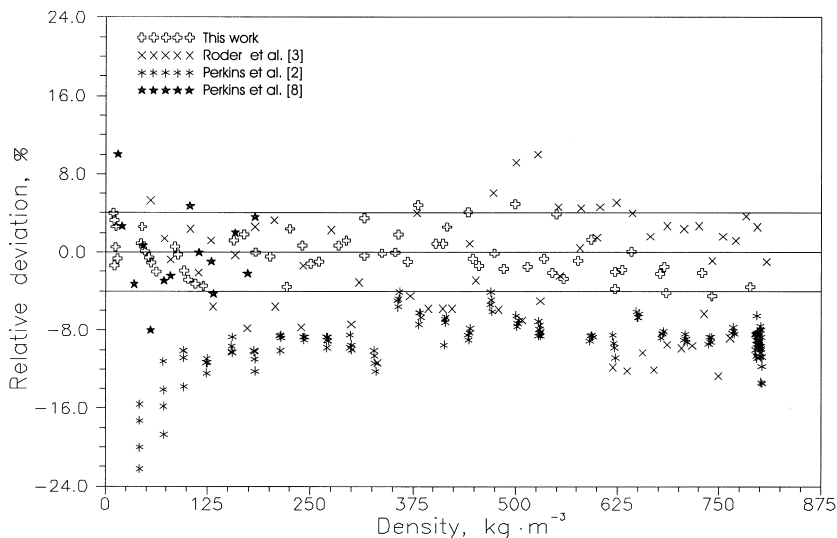


Fig. 7. Deviations of the thermal diffusivity of argon compared to the NIST SRD Database 14 [6].

large errors, with a maximum deviation of -24% . Although most of the data of Roder et al. [3] and of Perkins and Friend et al. [8] show deviations of less than 4% , a significant number still deviate from the correlation by more than 4% , some with maximum deviations as large as -12% . In the case of the results reported here, however, nearly all deviate by less than $\pm 4\%$ from the computed values.

To derive ideal-gas specific heats for argon, and thus make a comparison to theoretical values, the low-density data were extrapolated linearly to zero density for each isotherm. The experimental ideal-gas specific heat values are indicated in Fig. 8, and deviations from the theoretical value of $520.7 \text{ J} \cdot \text{kg}^{-1} \cdot \text{K}^{-1}$ [6] are shown in Fig. 9. The maximum deviation is about 3% , with a standard deviation of less than 2% .

A comparison of experimental isobaric specific heats as a function of density, calculated using the experimentally determined thermal conductivity and thermal diffusivity results and compared to values derived from the NIST SRD Database 14 [6], is shown in Fig. 6. The maximum deviation is about $\pm 4\%$, with a standard deviation of approximately 2% .

4.3. Discussion

The thermal conductivity, thermal diffusivity, and isobaric specific heat values listed in Table II indicate uncertainties of less than 1% for

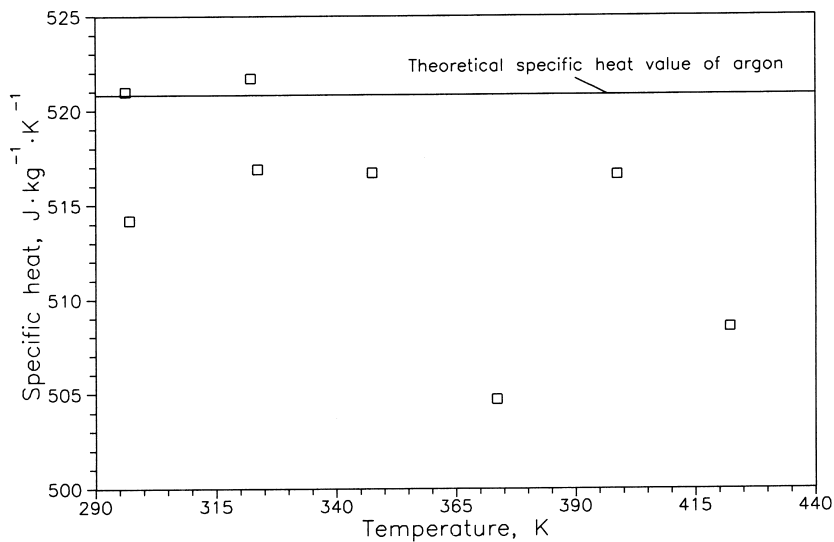


Fig. 8. Ideal-gas specific heat of argon obtained by low-density extrapolation; present work.

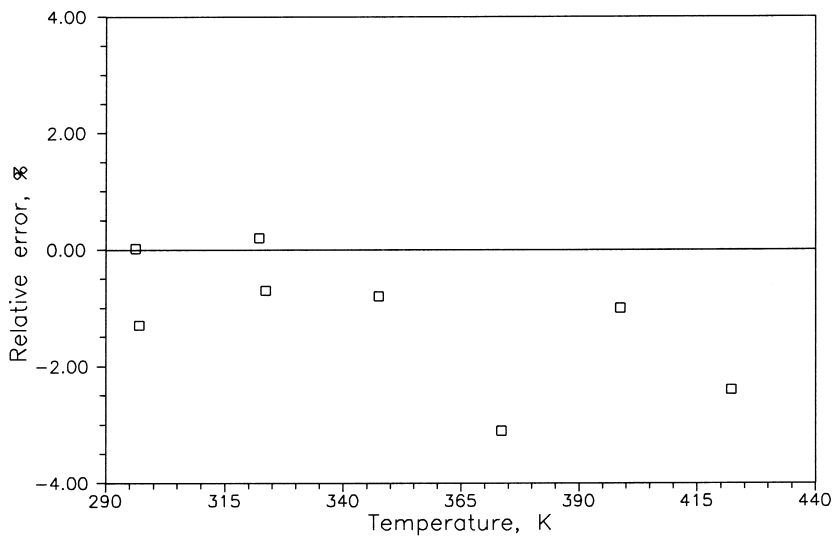


Fig. 9. Deviations of ideal-gas specific heat of argon from theory; present work.

thermal conductivity and 4% for thermal diffusivity and specific heat at a confidence level of 95%. The corrections for the bridge imbalance and the temperature variation of thermal diffusivity were found to be essential to the successful determination of the thermal diffusivity and hence the specific heat when the density is available.

It is therefore useful to examine the necessary correction procedures in some detail. As mentioned in Section 2, the temperature coefficient of the measured thermal conductivity near the bath temperature and test pressure is obtained by applying several heating powers to measure the thermal conductivity at different reference temperatures. The thermal conductivity and thermal diffusivity of the fluid corresponding to the initial base temperature are then obtained by using Eq. (8). However, a systematic and nearly constant temperature “offset” still exists in the thermal diffusivity results. To obtain this correction the temperature rise at a given instant is linearly regressed as a function of $q/(4\pi\lambda_0)$ and the intercept at zero power determined. This correction thus represents a zero-time effective time bridge imbalance.

To demonstrate the influence of this correction to measurements of thermal diffusivity, consider the data from Ref. 3 at 298.35 K and 65.51 MPa, for points 1121–1132. On close examination the data all show systematic variations with power; with an increase in q , values of α appear to approach a constant asymptotically. From these measurements the temperature coefficient of thermal conductivity can be determined; thus, $\chi = -0.00356 \text{ K}^{-1}$, $\Delta T_1 = 3.9771 \text{ K}$ ($t_1 = 0.15 \text{ s}$), and $\Delta T_2 = 5.1344 \text{ K}$ ($t_2 = 1.0 \text{ s}$) with $\lambda_0 = 0.05434 \text{ W} \cdot \text{m}^{-1} \cdot \text{K}^{-1}$ for $q = 0.41638 \text{ W} \cdot \text{m}^{-1}$ at point 1132. Equation (11) therefore indicates that the “true” value of thermal diffusivity is about +6.5% over the value determined by Eq. (4) and reported in Ref. 3. After applying the corrections, the adjusted results still display systematic variations in α with q (Fig. 10a); there is an apparent increase in α with q . This may be taken to suggest still further errors in the determination of the circuit balance and its “effective” zero-time temperature-difference equivalent. Equation (9) may therefore be used to determine those values necessary (of the order of 10s of mK) to obtain “corrected,” and hence power-independent, thermal diffusivity values. Values corrected in this manner indicate a reproducibility of the order of 1% (Fig. 11). The temperature correction necessary to obtain this was only $-10.52 \pm 0.07 \text{ mK}$.

Further illustration may be seen by considering the data from this paper, points A20_0A2 to A20_0D4 (Fig. 10b). Here, again, the data were first evaluated via Eq. (4) and then corrected for the temperature variation in thermal conductivity and then to determine the effective temperature imbalance of the bridge at time 0: $8.76 \pm 0.04 \text{ mK}$. In Fig. 11 it can be seen

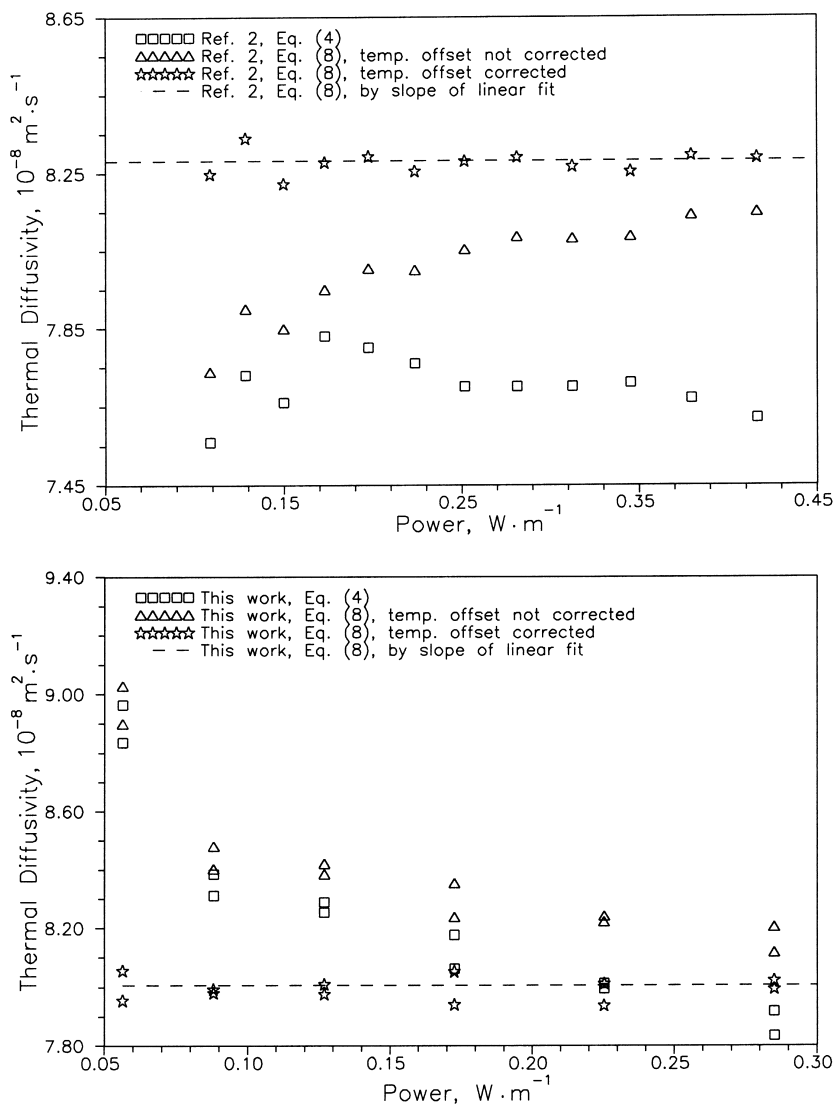


Fig. 10. Experimental thermal diffusivity of argon before and after correction: (a) Ref. 3; (b) this work.

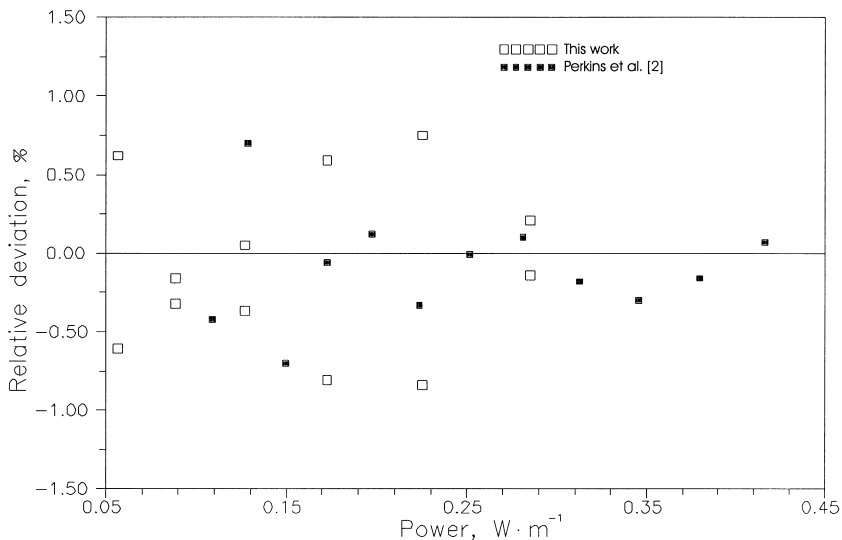


Fig. 11. Deviations in the thermal diffusivity from values obtained after corrections for the temperature coefficient and bridge “zero” balance offset.

that the reproducibility of both sets of thermal diffusivity data is comparable and of the order of 1%.

The importance of this influence emphasizes the need for a very accurate bridge balance and the use of techniques, such as above, to determine the equivalent “zero”-time bridge imbalance in the determination of precise values of thermal diffusivity using the transient hot-wire technique.

To demonstrate the influence of temperature offset on the thermal conductivity values in this work, the deviations of the thermal conductivity at a bath temperature obtained independently before and after correcting the temperature offset from that derived using the fitting method above are shown in Fig. 12 for points A20_0A2 to A20_0D4. We can see that the thermal conductivity data deviate by less than 0.2% from the data obtained with the fitting method despite any correction of the temperature offset. These results indicate that the reproducibility for thermal conductivity is within 0.5%, and the influence of the temperature offset on the thermal conductivity in the present measurements can be ignored.

4.4. Thermal Conductivity at Low Densities

Recent low-density, $1 < \rho < 125 \text{ kg} \cdot \text{m}^{-3}$, thermal conductivity measurements [14] utilized the same instrument to obtain both transient and

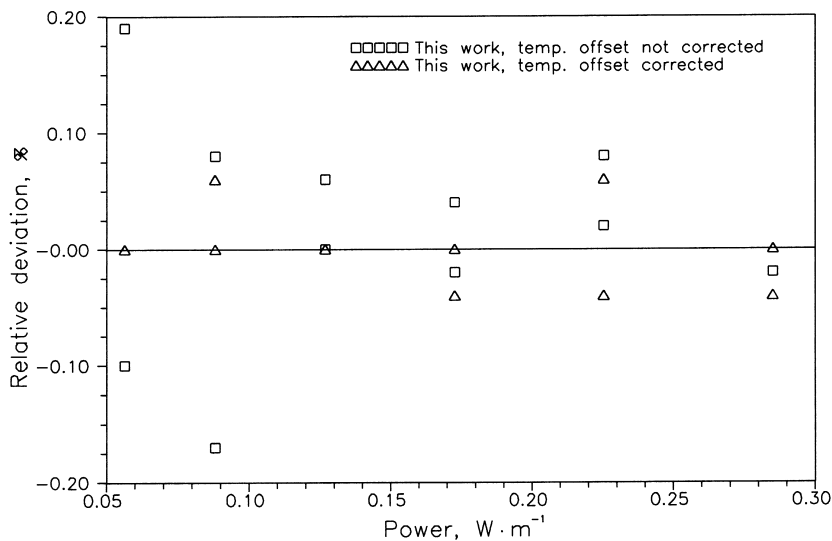


Fig. 12. Deviations in the independently determined thermal conductivity at the reference temperature compared to those obtained directly from experiment.

steady-state hot-wire data. Similar measurements were also made near 296.2, 323.6, and 347.5 K for a variety of power levels (Table II). First, the thermal conductivity at the preset cell temperature and pressure were measured. These results were obtained as a function of power (i.e., reference temperature) and were linearly regressed to obtain the temperature

Table IV. Thermal Conductivity of Argon at Low Densities from This Work ($\rho < 125 \text{ kg} \cdot \text{m}^{-3}$)

T (K)	P (kPa)	ρ ($\text{kg} \cdot \text{m}^{-3}$)	λ ($\text{W} \cdot \text{m}^{-1} \cdot \text{K}^{-1}$)	χ (K^{-1})
300.00	333	5.34868	0.01787 ^S	0.002745
300.00	333	5.34868	0.01780 ^T	0.001679
300.00	333	5.34868	0.01783	0.001791
300.00	882	14.1998	0.01811	0.001597
300.00	3757	61.4440	0.01924	0.001419
300.00	7106	117.975	0.02071	0.000942
320.00	851	12.8224	0.01900	0.002913
320.00	3744	57.0183	0.02017	0.002101
320.00	7247	111.457	0.02152	0.001292
340.00	864	12.2383	0.01970	0.003696
340.00	3884	55.4013	0.02087	0.003037
340.00	7235	103.737	0.02221	0.003028

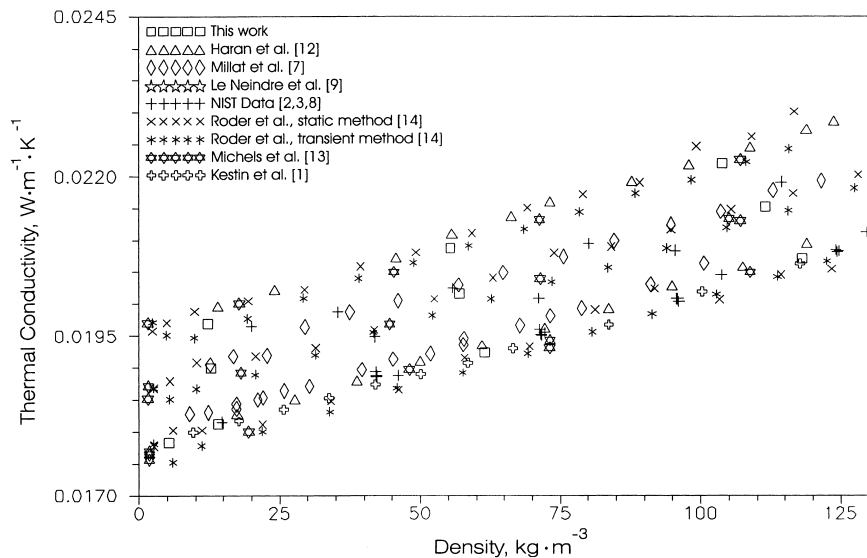


Fig. 13. The thermal conductivity of argon at low densities ($0 < \rho < 125 \text{ kg} \cdot \text{m}^{-3}$) from different literature sources as a function of density for the isotherms of 300, 320, and 340 K.

coefficient of thermal conductivity, χ , at the temperature of the thermostat, T_0 . Then, with the expression $\lambda = \lambda_0(1 + \chi \Delta T)$, the nominal thermal conductivity, along the isotherms 300, 320, and 340 K, were evaluated with the determined χ as listed in Table IV. Using the same determined values of χ , the thermal conductivity values from the other literature sources noted were also corrected to the nominal 300, 320, and 340 K isotherms (Fig. 13).

The thermal conductivity values in the density range $5 < \rho < 125 \text{ kg} \cdot \text{m}^{-3}$ determined here were then fit by the expression

$$\lambda = A\rho + B \quad (26)$$

with the linearly regressed coefficients shown in Table V. The thermal conductivity results from all other sources were then compared to the

Table V. Coefficient for Linear Regression $\lambda = A\rho + B$

T (K)	A ($\text{W} \cdot \text{m}^2 \cdot \text{kg}^{-1} \cdot \text{K}^{-1}$)	B ($\text{W} \cdot \text{m}^{-1} \cdot \text{K}^{-1}$)
300.00	2.48592×10^{-5}	0.0177535
320.00	2.55210×10^{-5}	0.0186844
340.00	2.74247×10^{-5}	0.0193584

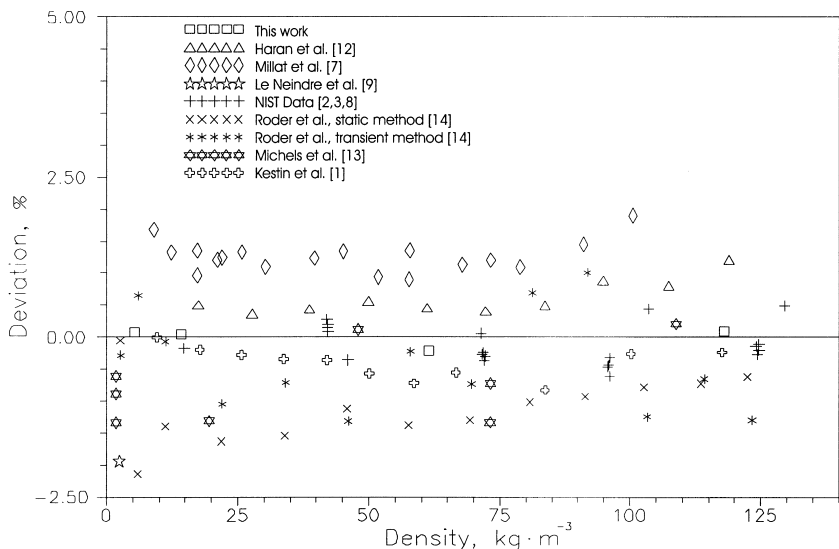


Fig. 14. Deviations in the thermal conductivity of argon along the isotherm of 300 K from Eq. (26).

values given by Eq. (26) and the deviations, as functions of density, are shown in Fig. 14–16. From this comparison it can be seen that deviations in excess of $\pm 1\%$ are few and the results distribute evenly about the baseline.

The steady-state method [14] was also attempted for a few measurements near 296 K at 0.333 MPa with wire powers of 0.056582 and 0.12747 $\text{W} \cdot \text{m}^{-1}$ using the same instrument as for the measurements using the transient method. The temperature rise of the hot wire for these measurements is shown in Fig. 17 as a function of time. The steady-state temperature rises are those points where the thermal wave reaches the outer cell boundary, i.e., about 3 and 7.5 K. The thermal conductivity was obtained via the usual expression for conduction between infinite concentric cylinders,

$$\lambda = \frac{q \ln\left(\frac{b}{a}\right)}{2\pi(T_1 - T_2)} \quad (27)$$

where b is the radius of the cell enclosure, a is the radius of the wire, and $\Delta T = T_1 - T_2$ is the temperature difference between the wire and its surrounding cell wall at steady state. The measured thermal conductivity corresponds to a mean temperature of [14]

$$\bar{T} = (T_1 + T_2)/2 \quad (28)$$

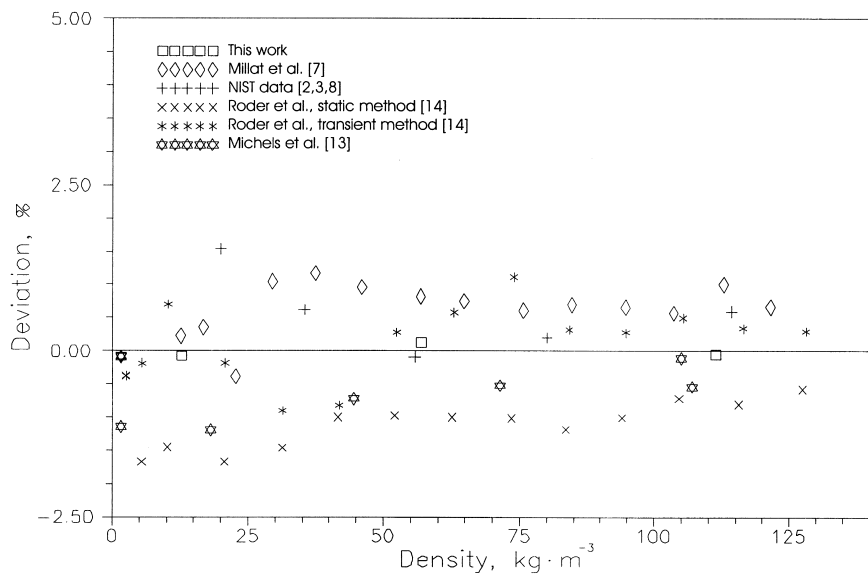


Fig. 15. Deviations in the thermal conductivity of argon along the isotherm of 320 K from Eq. (26).

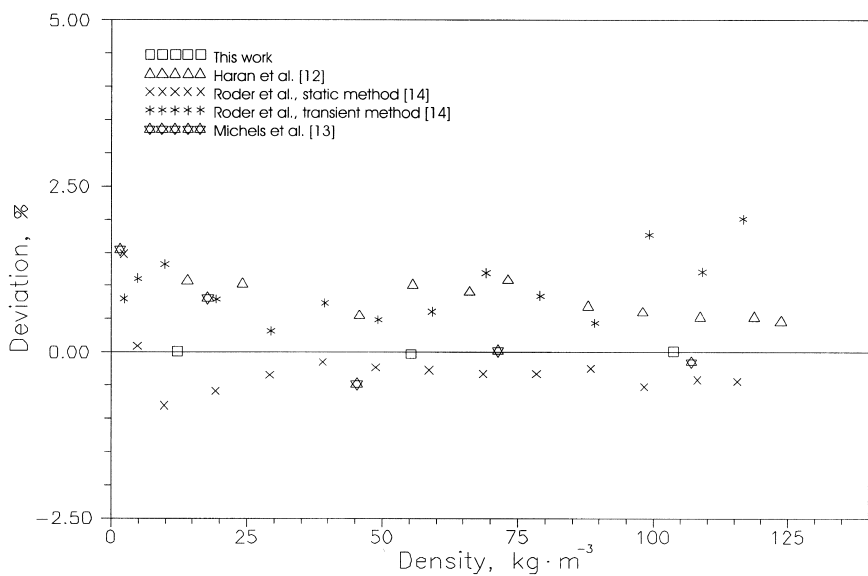


Fig. 16. Deviations in the thermal conductivity of argon along the isotherm of 340 K from Eq. (26).

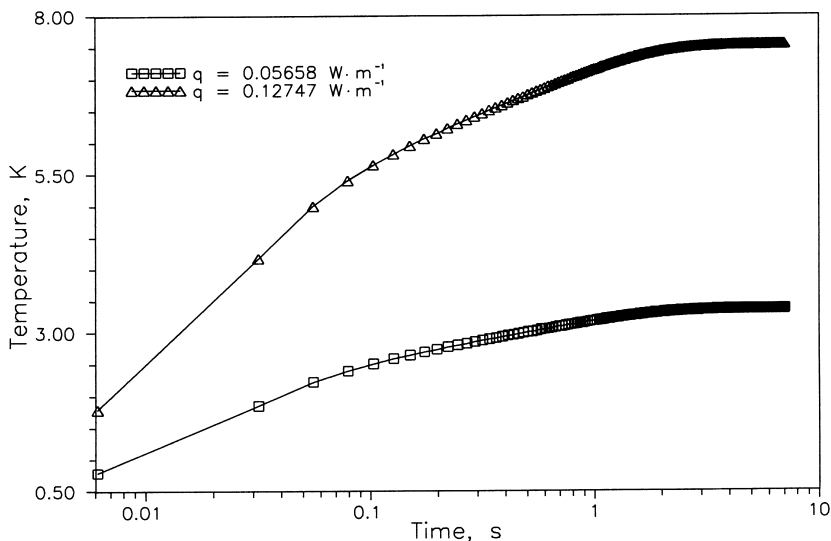


Fig. 17. Temperature rise of the hot wire as a function of time for both steady-state and transient methods.

The hot-wire temperature rises, shown in Fig. 17, were also processed as transients using Eq. (1), and the thermal conductivity values determined after the necessary appropriate corrections. The values obtained by both methods are listed in Table II, labeled with superscripts S and T, respectively. As with the transient measurements, the measurements were all processed to determine the temperature coefficient of thermal conductivity and the values at the nominal 300 K isotherm evaluated as listed in Table IV. It can be seen that the difference between the thermal conductivity results obtained with static and those obtained with transient methods is within the uncertainty of measurement.

5. CONCLUSION

In summary, the thermal conductivity and thermal diffusivity of argon in the range of 296 to 425 K and up to 61 MPa were measured using a transient hot-wire instrument. A new analysis of the influence of temperature-dependent properties and residual bridge imbalance was used to obtain thermal conductivities with an uncertainty of less than 1% and thermal diffusivities and derived specific heats with an uncertainty of less than 4%.

The present measurements of thermal conductivity were employed to establish a correlation equation in the range of 296 to 425 K and up to

61 MPa with an uncertainty of $\pm 2\%$. The thermal conductivity data from all other data sources are in excellent agreement with this correlation, with uncertainties of less than 3%.

The thermal diffusivity results of both Roder et al. [3] and Perkins et al. [2] should be investigated for the influence of the temperature coefficient of the thermal conductivity and bridge “zero” offset, or imbalance, to obtain more precise values of thermal diffusivity.

ACKNOWLEDGMENT

This work was performed under a program of studies funded by the Natural Sciences and Engineering Research Council of Canada, under NSERC OPG 8859-2000.

REFERENCES

1. J. Kestin, R. Paul, A. A. Clifford, and W. A. Wakeham, *Physica A* **100**:346 (1980).
2. R. A. Perkins, H. M. Roder, and C. A. Nieto de Castro, *J. Res. Natl. Bur. Stand.* **96**:247 (1991).
3. H. M. Roder, R. A. Perkins, and C. A. Nieto de Castro, *Int. J. Thermophys.* **10**:1141 (1989).
4. J. J. Healy, J. J. de Groot, and J. Kestin, *Physica C* **82**:392 (1976).
5. L. Sun, Ph.D. dissertation (Dept. Mech. Eng., University of New Brunswick, Fredericton).
6. D. G. Friend, *Standard Reference Database 14, Mixture Property Database* (NIST14) Version 9.09 (Institute of Standards and Technology, Gaithersburg, MD, 1993).
7. J. Millat, M. Mustafa, M. Ross, W. A. Wakeham, and M. Zalaf, *Physica A* **145**:461 (1987).
8. R. A. Perkins, D. G. Friend, H. M. Roder, and C. A. Nieto de Castro, *Int. J. Thermophys.* **12**:965 (1991).
9. B. Le Neindre, *Int. J. Heat Mass Transfer* **15**:1 (1972).
10. U. V. Mardolcar, C. A. Nieto de Castro, and W. A. Wakeham, *Int. J. Thermophys.* **7**:259 (1986).
11. M. Yorizane, S. Yoshimura, H. Masuoka, and H. Yoshida, *Ind. Eng. Chem. Fundam.* **22**:454 (1983).
12. N. Haran, G. C. Maitland, M. Mustafa, and W. A. Wakeham, *Ber. Bunsenges. Phys. Chem.* **87**:657 (1983).
13. A. Michels, J. V. Sengers, and L. J. M Van der Klundert, *Physica* **29**:149 (1963).
14. H. M. Roder, R. A. Perkins, A. Laesecke, and C. A. Nieto de Castro, *J. Res. Natl. Bur. Stand.* **105**:221 (2000).